

# Regulation and Surveillance of Normal and 3'-Extended Forms of the Yeast Aci-reductone Dioxygenase mRNA by RNase III Cleavage and Exonucleolytic Degradation\*

Received for publication, May 31, 2005, and in revised form, June 20, 2005  
Published, JBC Papers in Press, June 20, 2005, DOI 10.1074/jbc.M505913200

Cindy Zer‡ and Guillaume Chanfreau§

From the Department of Chemistry and Biochemistry and the Molecular Biology Institute, University of California, Los Angeles, California 90095

**Aci-reductone dioxygenases are key enzymes in the methionine salvage pathway. The mechanisms by which the expression of this important class of enzymes is regulated are poorly understood. Here we show that the expression of the mRNA encoding the yeast aci-reductone dioxygenase *ADII* is controlled post-transcriptionally by RNase III cleavage. Cleavage occurs in a large bipartite stem loop structure present in the open reading frame region of the *ADII* mRNA. The *ADII* mRNA is up-regulated in the absence of the yeast orthologue of RNase III Rnt1p or of the 5' → 3' exonucleases Xrn1p and Rat1p. 3'-Extended forms of this mRNA, including a polycistronic mRNA *ADII-YMR010W* mRNA, also accumulate in cells lacking Rnt1p, Xrn1p, and Rat1p or the nuclear exosome component Rrp6p, suggesting that these 3'-extended forms are subject to nuclear surveillance. We show that the *ADII* mRNA is up-regulated under heat shock conditions in a Rnt1p-independent manner. We propose that Rnt1p cleavage targets degradation of the *ADII* mRNA to prevent its expression prior to heat shock conditions and that RNA surveillance by multiple ribonucleases helps prevent accumulation of aberrant 3'-extended forms of this mRNA that arise from intrinsically inefficient 3'-processing signals.**

zymes has important biomedical implications. One product of the off-pathway is carbon monoxide (Fig. 1), which is toxic and also a candidate for a new class of neural messengers (3). The other product, methyl propionate, is cytotoxic and has been implicated in pathogenicity in plants (1). In addition, the rodent homologue of ARD, *ALP1*, is regulated by androgen in prostate cells and down-regulated in prostate cancer cell lines (4). Overexpression of *ALP1* also leads to prostate cell death, suggesting that *ALP1* may have an important role in prostate cancer progression by regulating the death of cancerous cells (4). Understanding the regulation of genes encoding ARD enzymes is therefore essential to the understanding of the metabolism of biomolecules with important biological functions and of the mechanisms of prostate cancer progression.

In this study, we show that the mRNA encoding the yeast orthologue of ARD, *ADII*, is subject to post-transcriptional cleavage by the yeast ribonuclease III Rnt1p. Rnt1p is a double-stranded RNA endonuclease previously involved in the processing of stable RNA precursors (5–8) as well as in the degradation of some mRNAs (9–11). We show that Rnt1p cleavage and degradation by various exonucleases control *ADII* mRNA levels and prevent the accumulation of 3'-extended forms of this mRNA. We also show that the *ADII* mRNA is induced in heat shock conditions. We propose that Rnt1p cleavage and/or degradation by exonucleases helps prevent the accumulation of *ADII* mRNA prior to heat shock conditions and that these ribonucleolytic pathways provide a mechanism to eliminate 3'-extended forms that arise from poor 3'-end processing signals present at the end of the *ADII* gene.

## MATERIALS AND METHODS

Strains used in this study have been described previously (9, 12, 13). RNA preparation and Northern analysis were performed according to (9, 12). [<sup>32</sup>P]dCTP-labeled probes were generated from PCR products spanning the following regions: walk 1, from 400 to 200 nucleotides upstream from the *ADII* ORF; walk 3, *ADII* translation initiation codon to position 200 of the *ADII* ORF; walk 4, from position 200 to position 400 of the *ADII* ORF; walk 8, from 100 nucleotides downstream from the *ADII* ORF to 175 nucleotides upstream from the *YMR010W* initiation codon; *YMR010W*, from 250 nucleotides downstream from the *YMR010W* translation initiation codon to 450 nucleotides upstream from the *YMR010W* translation termination codon.

Oligonucleotide-mediated RNase H mapping was performed according to (14). Oligonucleotides used for the RNase H mapping were as follows: oligo 1, 5'-GGCAATTAACCTCACTAAAGGCCCTGGCAGAAATTACC-3'; oligo 2, 5'-CGCGGATCCGGCAATTAACCTCACTAAAGGCCCTTAACCATCT AACTTTTGACC3-'; oligo 3, 5'-CCTGTTGATAGCTTGCC-3'; oligo 4, 5'-GGCAATTAACCTCACTAAAGGCCGTGATAAGGCTTTTGC-3'; oligo 5, 5'-GGCAATTAACCTCACTAAAGGCCGGAATGCAACAGTATGCG-3'; and oligo 6, 5'-CCCTATGATAGAGCCAGTCC-3'.

*In vitro* cleavage using recombinant Rnt1p or a catalytically inactive mutant, E320K, and mapping of the cleavage sites by primer extension were performed as described (8, 9). The ACA or short stem loop

Aci-reductone dioxygenase (ARD)<sup>1</sup> enzymes play important roles in methionine metabolism (Fig. 1). The prototype *Klebsiella pneumoniae* ARD enzyme catalyzes different reactions with the same substrate depending on the type of metal ion bound in its active site. With Ni<sup>2+</sup> (ARD in Fig. 1), the enzyme catalyzes the off-pathway oxidation of aci-reductone with formation of carbon monoxide (1). In the presence of Fe<sup>2+</sup> (ARD' in Fig. 1), it catalyzes the on-pathway oxidation to ketoacid and formate (1). Thus, the same protein can act as different enzymes, depending on the type of metal bound to its active site. The key role of this enzyme in the methionine salvage pathway is conserved from bacteria to mammals (2). The regulation of the gene expressing ARD en-

\* This work was supported by National Institutes of Health Grant GM61518 (to G. C.). The costs of publication of this article were defrayed in part by the payment of page charges. This article must therefore be hereby marked "advertisement" in accordance with 18 U.S.C. Section 1734 solely to indicate this fact.

‡ Present address: UCLA David Geffen School of Medicine, Membrane Biology Laboratory/WLA VAMC, 11301 Wilshire Blvd., Los Angeles, CA 90073.

§ To whom correspondence should be addressed: Dept. of Chemistry and Biochemistry, University of California, Box 951569, Los Angeles, CA 90095-1569. Tel.: 310-825-4399; Fax: 310-206-4038; E-mail: guillom@chem.ucla.edu.

<sup>1</sup> The abbreviations used are: ARD, aci-reductone dioxygenase; ORF, open reading frame.

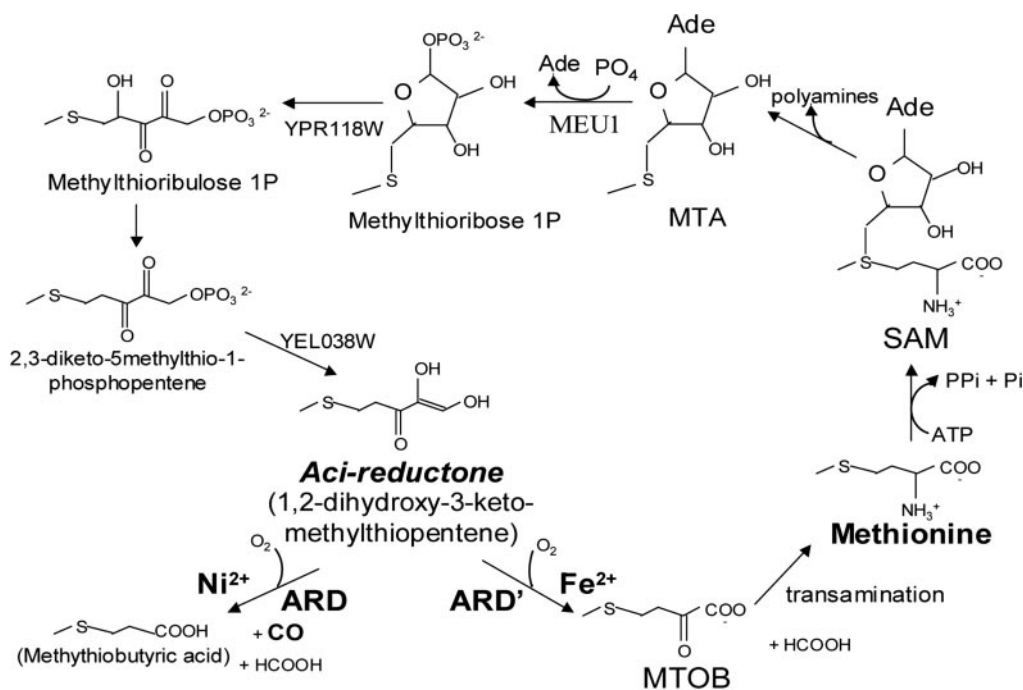


FIG. 1. **The methionine salvage pathway.** The steps at which the two forms of the aci-reductone dioxygenase enzymes are involved are indicated. *MTA*, methylthioadenosine; *SAM*, S-adenosylmethionine; *MTOB*, 4-methylthio-2-oxobutanoic acid. The pathway is summarized from the studies in (2).

deletion ( $\Delta$ SL) mutations were generated *in vivo* using the delitto perfetto method (15). After insertion of these mutations in the *ADII* chromosomal locus, *in vitro* transcription templates for the mutant substrates were generated by PCR using primers spanning the mutagenized region.

## RESULTS

*The YMR009W mRNA Encoding the Yeast Aci-reductone Dioxygenase Adi1p Is Expressed in a Complex Pattern and Is Up-regulated in the Absence of Yeast RNase III*—We previously analyzed whole genome gene expression in cells lacking the yeast orthologues of RNase III Rnt1p by microarrays (11). Among the candidates identified through our microarray studies was the *YMR009W* mRNA, which was up-regulated 3-fold in cells lacking Rnt1p. The *YMR009W* gene encodes a protein with significant sequence similarity to the *K. pneumoniae* ARD and to the rodent ARD enzyme ALP1 (1, 4, 16). The ARD enzymes are conserved between bacteria, yeast, and mammals (4). The involvement of the gene product of *YMR009W* in methionine metabolism was demonstrated experimentally (17). We therefore decided to investigate the potential regulation of this member of an important class of enzymes by Rnt1p. Because the *ARD* or *ALP* acronyms were already used, we called the gene and protein product of *YMR009W* *ADII* and *Adi1p*, respectively, for aci-reductone dioxygenase 1.

To gain further insight into the potential control of the expression of *Adi1p* by Rnt1p, we analyzed the expression of the *ADII* mRNA in wild-type cells and in cells lacking Rnt1p (*rnt1* $\Delta$ ) by Northern blot analysis. The *ADII* gene is located near a downstream gene, *YMR010W* (Fig. 2A). We first hybridized membranes containing RNAs extracted from both strains with a probe that hybridizes against the *ADII* mRNA (Fig. 2A, walk 4 probe). In addition to the most abundant band, which corresponds to the *ADII* mRNA (see below), this probe also detected three additional minor species, two of which migrated slower and one that migrated faster. Note that the faster migrating species is found in equal abundance in wild-type and *rnt1* $\Delta$  strains, serving as an internal control. This analysis confirmed the higher abundance of the *ADII* mRNA in RNAs

extracted from the *rnt1* $\Delta$  cells (Fig. 2A). To further characterize these different species, we synthesized additional probes derived from PCR products of different regions of the *ADII*-*YMR010W* loci. The walk 1 probe hybridizes upstream from the *ADII* ORF, walk 3 hybridizes within the *ADII* ORF, and walk 8 hybridizes within the intergenic *ADII*-*YMR010W* region (Fig. 2A). In addition, we also synthesized a probe hybridizing to the *YMR010W* mRNA. All of these probes detected the slower migrating species, suggesting that it corresponds to an extended species containing both the *ADII* and *YMR010W* ORFs (Fig. 2B). The profile of RNAs detected by the walk 3 probe was similar to that of the walk 4 probe (Fig. 2B). The walk 1 probe, which hybridizes upstream from the *ADII* ORF, detected all but the faster migrating species. Note that this probe hybridizes 400 to 200 nucleotides upstream from the *ADII* ORF, suggesting that the *ADII* transcripts have an unusually long 5'-untranslated region. Hybridization with the *YMR010W* probe revealed the *YMR010W* mRNA and also detected the largest species (Fig. 2B). The faster migrating species was detected only by the walk 3 and walk 4 probes (Fig. 2B), suggesting that it does not contain much additional sequence besides the *ADII* ORF.

To investigate the status of polyadenylation of species that accumulate in cells lacking Rnt1p, we purified polyadenylated RNAs using oligo(dT) affinity and compared the profiles of RNAs hybridizing to the walk 4 probe in total and poly(A) RNA samples (Fig. 2C). This experiment showed that all species that accumulate in the *rnt1* $\Delta$  strain are polyadenylated. The largest species was not as well enriched as other species in the poly(A)-purified RNAs. This might mean that these long species are heterogeneously polyadenylated or that they were somehow underrepresented during the poly(A) purification because of their long sizes.

Although the expression of most of these forms is higher overall in the *rnt1* $\Delta$  strain, the same bands are observed in the wild-type strain (see Fig. 2B, walk 4 probe), suggesting that this complex pattern of expression is representative of species expressed in the wild-type strain. We further characterized

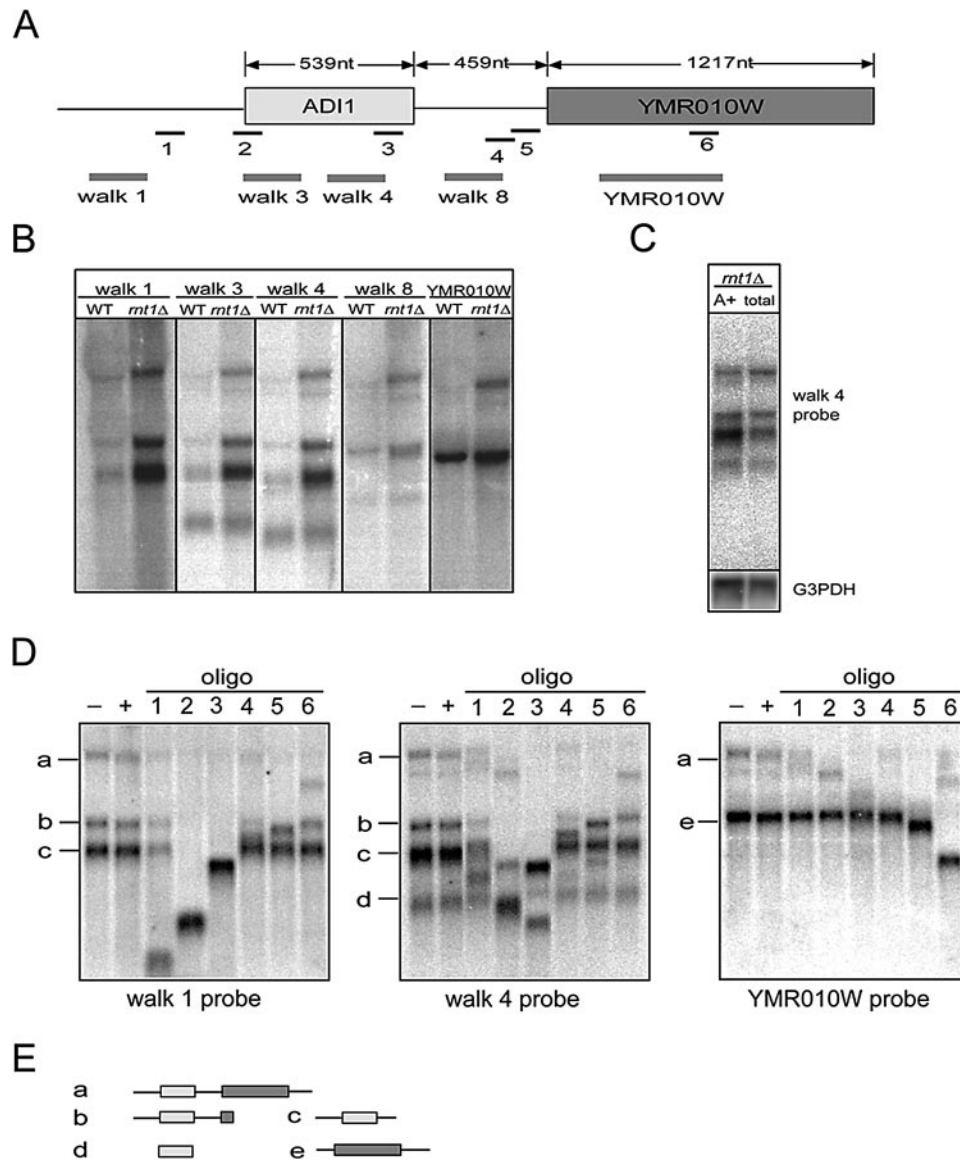


**FIG. 2. Northern blot analysis of the expression of the *ADI1* and *YMR010W* mRNAs and characterization of extended species.** *A*, genomic structure of the *YMR009W/ADI1-YMR010W* genomic regions. Boxes indicate the open reading frames. The exact sites of transcription initiation and termination are unknown. Gray lines indicate the regions corresponding to the different probes used, whereas black lines indicate the region where the different oligonucleotides used for the RNase H mapping hybridize. *nt*, nucleotides. *B*, Northern analysis of the *ADI1* and *YMR010W* mRNAs in wild-type (WT) and *rnt1Δ* cells. RNAs extracted from wild-type and *rnt1Δ* strains were fractionated on an agarose Northern blot, transferred to a nylon membrane, and probed with radiolabeled probes corresponding to the genomic regions indicated in panel *A*. *C*, polyadenylation status of the *ADI1* mRNA species found in the *rnt1Δ* strain. Total RNA or poly(A)-selected RNAs (A+) extracted from *rnt1Δ* were loaded on an agarose gel and analyzed by Northern blot. *D*, RNase H mapping of the species expressed from the *ADI1-YMR010W* genomic region. Minus sign (-), mock treatment without RNase H; plus sign (+), treatment with RNase H but no oligonucleotide. Other reactions included the indicated oligonucleotides and RNase H. *E*, schematic representation of the different species mapped. Legends are as for panel *A*.

these species in RNAs extracted from the *rnt1Δ* strain because their higher abundance made the analysis easier. We performed RNase H digestion using oligonucleotides hybridizing to different areas of the *ADI1-YMR010W* genomic region (Fig. 2A), followed by hybridization using three different probes. Oligo 1 hybridizes upstream from the *ADI1* ORF, oligos 2 and 3 hybridize to the 5'- and 3'-ends of the *ADI1* ORF, respectively, and oligos 4 and 5 hybridize to the intergenic *ADI1-YMR010W* region, whereas oligo 6 hybridizes to the *YMR010W* mRNA (Fig. 2A).

In agreement with the pattern of hybridization observed in Fig. 2B, band *a* in Fig. 2D is clearly downshifted with oligos 2 and 6, showing that it is a long RNA species that spans the *ADI1* and *YMR010W* ORFs. When digested with oligos 2 or 3 and probed with the walk 1 probe, bands *a*, *b*, and *c* (Fig. 2D) disappeared and a single small species appeared, which

showed that bands *a*, *b*, and *c* have the same 5'-end. However, bands *b* and *c* (Fig. 2D) do not have the same 3'-end. The difference in the 3'-end of these two RNAs most likely lies in the region between oligo 3 and oligo 4, as band *b* (Fig. 2D) is digested with oligos 4 and 5, whereas band *c* is unaffected (walk 1 and walk 4 probes). In contrast, oligo 3, which hybridizes upstream from oligo 4, digests these two bands completely. In agreement with the previously described hybridization pattern (Fig. 2B), band *d* (Fig. 2D) is a very short RNA that contains mostly sequences of the *ADI1* ORF. It is only detected by the walk 3 and walk 4 probes (which hybridize to the *ADI1* ORF) and it is downshifted only when digested by oligos 2 and 3. Band *e* (Fig. 2D) is clearly the mRNA of *YMR010W*, as it is only digested by oligos 5 and 6.

Overall, these results show that at least five transcripts are generated from the *ADI1-YMR010W* genomic region (Fig. 2E)

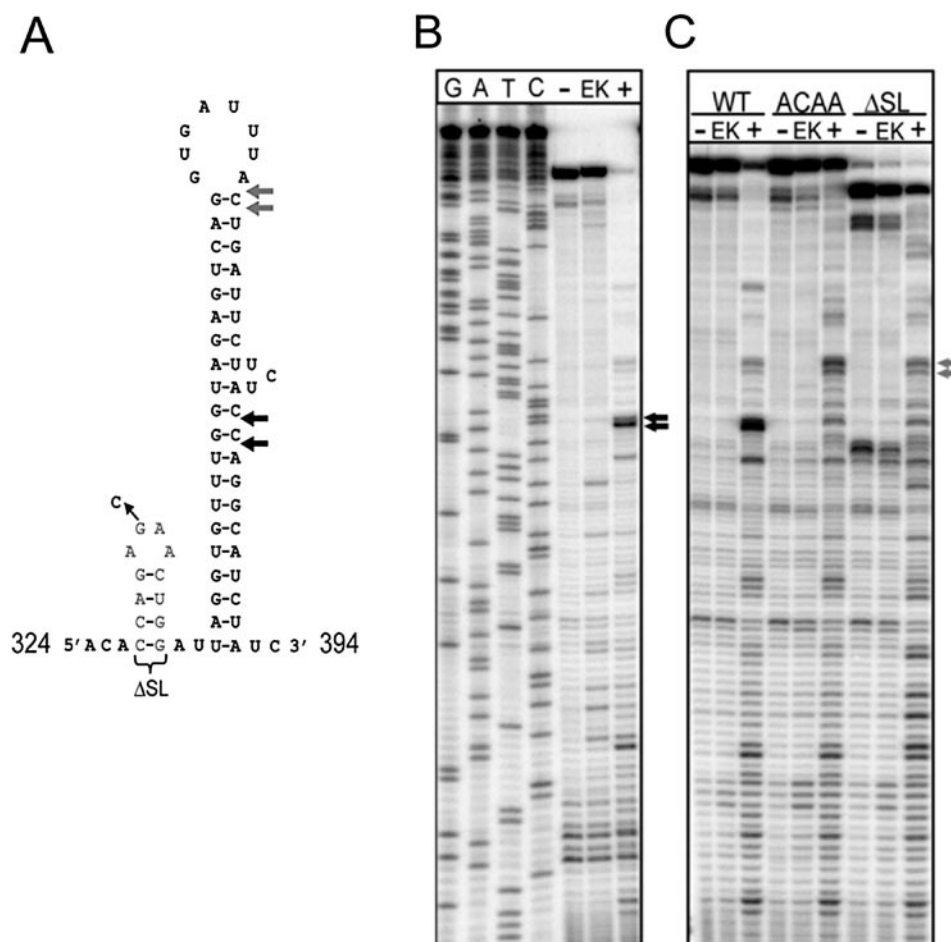


FIG. 3. *In vitro* cleavage of the *ADI1* mRNA by Rnt1p. **A**, predicted secondary structure of a portion of the *ADI1* mRNA. Shown is the region between nucleotides 324 and 394 of the *ADI1* ORF and the predicted secondary structure. Also indicated are the stem loop deletion and the ACAA point mutations studied in panel **C**. Mapped cleavage sites are indicated in the secondary structure. *Black arrows* indicate the major cleavage site observed with the wild-type substrate, whereas *gray arrows* indicate the major cleavage site mapped with the ACAA mutant. **B**, *in vitro* cleavage of the wild-type *ADI1* model substrate by recombinant Rnt1p. *In vitro* transcribed mRNA was incubated with buffer and recombinant wild-type Rnt1p (+), buffer and recombinant E320K Rnt1p mutant (*EK*), or buffer alone (–), and primer extension was performed to map the cleavage site(s), run in parallel with a sequencing ladder. **C**, *in vitro* cleavage of wild-type (*WT*) and mutant *ADI1* substrates by recombinant Rnt1p. Mutant substrates with a point mutation in the loop of the first hairpin (ACAA) or a deletion of the short stem loop ( $\Delta$ SL; see panel **A**) were incubated for *in vitro* cleavage with buffer, wild-type, or mutant recombinant Rnt1p. Legends are as in for panel **B**.

as follows: (i) the canonical *ADI1* mRNA (*band c*) with a rather long 5'-untranslated region; (ii) a shorter *ADI1* mRNA with shorter 5'-untranslated region and 3'-end (*band d*); (iii) a 3'-extended *ADI1* mRNA corresponding to *band b* that may partially extend onto the *YMR010W* ORF; (iv) the canonical *YMR010W* mRNA corresponding to *band e*; and (v) a dicistronic *ADI1-YMR010W* RNA corresponding to *band a*. Note that the walk 8 probe used in Fig. 2B detects a doublet of bands migrating faster than the dicistronic mRNA. Given the results of the hybridization with different probes and the RNase H mapping experiments, this doublet is likely to correspond to a mixture of *bands b* and *e* (Fig. 2, *D* and *E*), *i.e.* a mixture of 3'-extended *ADI1* mRNAs and *YMR010W* mRNAs that migrate very closely. These results show that the *ADI1* locus expresses a variety of transcripts and suggest that some of these transcripts arise from inefficient 3'-processing, which results in a fraction of transcripts that read through into the downstream ORF, *YMR010W*.

*A Model Transcript with Coaxially Stacked RNA Helices Present in the ADI1 mRNA Is Specifically Cleaved in Vitro by Recombinant Rnt1p*—Rnt1p usually cleaves double-stranded RNAs capped by tetraloop structures with the sequence AGNN (18, 19). We searched the sequence of *ADI1* mRNA for features that would resemble Rnt1p cleavage sites. Analysis of the the-

oretical secondary structure of the *YMR009W* mRNA using MFold (20, 21) predicted the existence of two sequential stem loop structures (Fig. 3A). The first stem loop is a small hairpin containing an AGAA tetraloop (*gray letters* in Fig. 3A) followed by a second longer hairpin with no apparent AGNN-type tetraloop. Stems capped by AGNN-type tetraloop structures are the major determinants of Rnt1p binding and cleavage (18, 22, 23). We hypothesized that this bipartite structure could reconstitute an RNase III cleavage site by stacking the small AGAA-containing stem onto the longer neighboring stem (Fig. 3A). This situation would be reminiscent of some processing signals present in small nucleolar RNA precursor substrates of Rnt1p (7, 8) or of some substrates of bacterial RNase III (24). To test if this bipartite stem loop could be cleaved efficiently *in vitro* using recombinant Rnt1p, we generated a model substrate containing these stem loops and incubated this substrate in the presence of recombinant Rnt1p or a catalytically inactive mutant (E320K). This experiment showed that Rnt1p cleaves this substrate efficiently *in vitro*, whereas no significant cleavage was observed with the catalytically inactive E320K mutant (Fig. 3B). Strikingly, the major cleavage generated by the wild-type protein was mapped 9–11 bp from the base of the long stem (Fig. 3, *A* and *B*, *black double arrows*). When the length of the helical region of the short stem loop (4 bp) was added to this

distance (9–11 bp), the cleavage site was found to be in agreement with the cleavage site selection rule of the enzyme, which normally cleaves 14–16 bp from terminal AGNN tetraloops (18). This observation suggests that the short stem loop coaxially stacks onto the longer stem to reconstitute a continuous helix that is recognized and cleaved by Rnt1p.

To further test that this bipartite RNA is a canonical target for yeast RNase III, we generated two mutant substrates. In the first substrate, the AGAA tetraloop is mutated to ACAA (Fig. 3A). This mutation strongly inhibits Rnt1p cleavage *in vitro* on canonical stem loop substrates (25). The second mutant carried a deletion of the short stem loop (Fig. 3A,  $\Delta SL$ ), which would be predicted to inhibit Rnt1p activity if the short AGNN-type stem loop directs the catalytic site onto the second stem. As shown in Fig. 3C, both mutations strongly inhibited Rnt1p activity, demonstrated by the large fraction of uncleaved substrate remaining, whereas >80% of the wild-type substrate was cleaved. This result shows that the short stem loop is important for cleavage in the second stem, as suggested by the mapping of the location of the cleavage site in the wild-type substrate. Surprisingly, some residual cleavage activity remained in these mutants. Although most cleavage at the normal site was inhibited, some cleavage was observed at a second site that was also observed in minor amounts with the wild-type substrate (labeled by a gray double arrow in Fig. 3, A and C). In the  $\Delta SL$  mutant we also observed numerous inefficient cleavages in the double-stranded region, suggesting that the AGNN short stem loop is not only required for efficient cleavage of the long stem but is also needed to dictate the specificity of cleavage within the second stem. In the absence of the short AGNN stem loop, the enzyme probably binds the double-stranded RNA with poor efficiency and cleaves it indiscriminately at multiple sites.

*The ADI1 mRNA Is Subject to Degradation by the Xrn1p and Rat1p Exonuclease, whereas 3'-Extended Species Are Degraded by Xrn1p, Rat1p, and Rrp6p*—To further investigate the post-transcriptional regulation of the *ADI1* mRNA, we analyzed its expression in strains carrying various exoribonuclease mutations. The 5'  $\rightarrow$  3' exonucleases Xrn1p and Rat1p have been shown to cooperate with Rnt1p in the processing or degradation of multiple RNA species (8, 9). Xrn1p is not essential, whereas Rat1p is encoded by an essential gene (26). Therefore we used a double mutant *xrn1 $\Delta$  rat1-1* strain (13) in which both exonuclease activities are inactivated after a shift to 37 °C. The nuclear exosome, a complex of 3'  $\rightarrow$  5' exonucleases, also cooperates with Rnt1p in the processing of multiple RNAs (27, 28). To investigate a potential function for the nuclear exosome in *ADI1* mRNA regulation, we used a mutant strain in which the nuclear exosome component Rrp6p is absent (*rrp6 $\Delta$* ). We studied the expression of the *ADI1* mRNA by Northern blot using RNAs extracted from these strains grown at 25 °C or shifted to 37 °C to inactivate the Rat1p exonuclease. Strikingly, in the wild-type strain we observed an increase of expression of the *ADI1* mRNA at 37 °C (Fig. 4), suggesting that the expression of the *ADI1* gene might be regulated by heat shock conditions. The faster migrating species did not show an increased expression at 37 °C. Given that this species has a shorter 5'-end than the regular mRNA (see Fig. 2), it is likely that this species is expressed from an alternative promoter that is not controlled by heat shock. We observed a stronger accumulation of the *ADI1* mRNA in the *xrn1 $\Delta$  rat1-1* strain than in the wild-type strain or in the individual mutant strains, suggesting that Xrn1p and Rat1p cooperate to degrade the *ADI1* mRNA (Fig. 4). This increase in the level of the *ADI1* mRNA was also apparent in the *xrn1 $\Delta$*  strain at 25 °C, showing that this exonuclease plays a major role in controlling the steady-state level

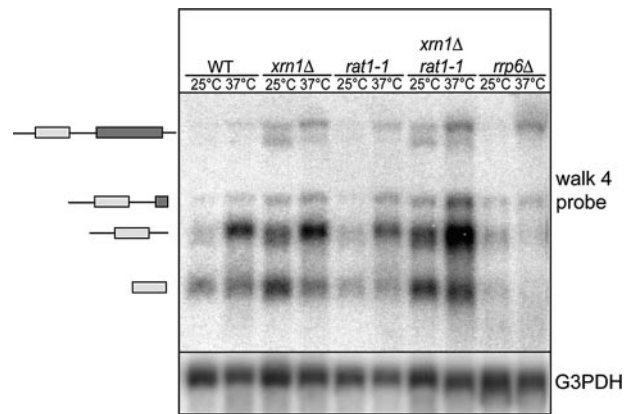


FIG. 4. Expression of the *ADI1* mRNAs in exonuclease mutant strains. RNAs extracted from the indicated strains grown at 25 °C, or shifted to 37 °C were analyzed by Northern blot using the walk 4 probe and the glyceraldehyde-3-phosphate dehydrogenase (*G3PDH*) probe. WT, wild-type.

of this mRNA (Fig. 4). In addition, we also observed an accumulation of the dicistronic species in the *xrn1 $\Delta$*  and *xrn1 $\Delta$ rat1-1* strains at both 25 and 37 °C, suggesting that these exonucleases also participate in the degradation of the polycistronic species that arise from poor 3'-end processing or transcription termination of the *ADI1* gene. We did not observe an induction of the *ADI1* mRNA at 37 °C in the *rrp6 $\Delta$*  strain (Fig. 4), which may be due to the fact that this strain is thermosensitive and that some indirect effect might prevent the induction of this gene at 37 °C. However, we observed a significant accumulation of dicistronic species in this strain, showing that the nuclear exosome also contributes to degradation of these species. Overall, these results show that multiple exonucleases cooperate in the degradation of normal and 3'-extended forms of the *ADI1* mRNA. Because the 3'-extended forms are present in the wild-type strain but accumulate only at low levels, we speculate that these species arise from intrinsically poor 3'-processing signals present downstream from the *ADI1* mRNA, which results in read-through transcripts in the downstream open reading frame. Multiple exoribonucleolytic pathways therefore contribute to the discarding of these aberrantly terminated or processed mRNAs.

*Effects of Heat Shock and the Short Stem Loop Deletion on the Expression of the ADI1 mRNA*—The previous experiment showed that the *ADI1* mRNA is up-regulated at 37 °C in the wild-type strain, suggesting that this mRNA might be induced under mild heat shock conditions. To further investigate this potential regulation, we shifted wild-type and *rnt1 $\Delta$*  cells to different temperatures and monitored the expression of the different *ADI1* transcripts (Fig. 5). This experiment confirmed the previous observation that the *ADI1* mRNA is induced at 37 °C and showed that this induction is also visible after a 15-min exposure to 42 °C (Fig. 5). This result shows that the *ADI1* mRNA is generally induced under heat shock conditions. This observation fits previous microarray data (29). We also noticed the appearance of the polycistronic *ADI1-YMR010W* transcript in wild-type cells that were heat-shocked at 42 °C (Fig. 5). The level of the *ADI1* mRNA also increased when the *rnt1 $\Delta$*  strain was shifted to 37 or 42 °C, showing that the increased expression upon heat shock occurs independently from Rnt1p activity. We also studied a strain expressing an in-frame chromosomal deletion of the short stem loop in the endogenous *ADI1* gene. This deletion is identical to the one studied *in vitro* in Fig. 3C. Strikingly, this deletion resulted in an increase of the expression of the *ADI1* mRNA and of the dicistronic *ADI1-YMR010W* RNA at 42 °C compared with the wild-type strain, but there was no

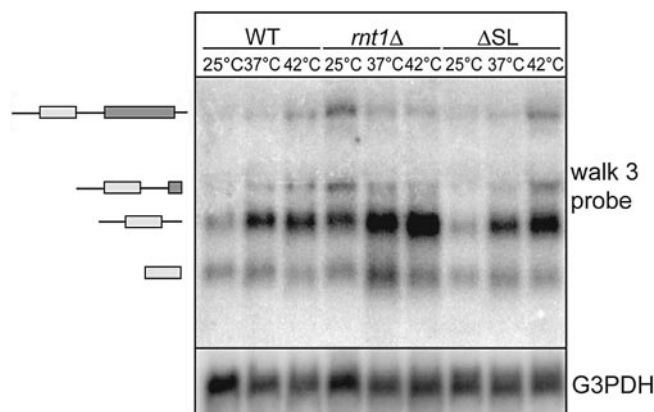


FIG. 5. Expression of the *ADI1* mRNA in heat shock conditions in wild-type (WT), *rnt1Δ*, and stem loop deletion ( $\Delta$ SL) strains. RNAs extracted from the indicated strains grown at 25 °C or shifted to 37 or 42 °C were analyzed by Northern blot using the walk 3 probe and the glyceraldehyde-3-phosphate dehydrogenase (*G3PDH*) probe.

significant increase at 25 °C compared with the wild-type strain. This result shows that deletion of the short stem loop partially phenocopies the absence of Rnt1p, at least at high temperatures. The lack of phenotype observed at 25 °C should be interpreted in the light of the result showing that deletion of this short stem loop does not completely abolish cleavage *in vitro* and results in a loss of specificity of the enzyme, which cleaved inefficiently and indiscriminately in the long stem structure of this substrate (Fig. 3C). Thus, it is possible that the residual nonspecific cleavage activity observed with this substrate *in vitro* is sufficient to provide the enzyme with sufficient activity at 25 °C to cleave this RNA and prevent its expression at normal temperatures. The stronger effect observed at higher temperatures might be due to the fact that a smaller fraction of the transcripts folds into the predicted secondary structure, abolishing the residual cleavage activity. In conclusion, these data show that the short stem loop deletion partially phenocopies the absence of Rnt1p and suggests that Rnt1p cleavage may help down-regulate the expression of the *ADI1* mRNA under conditions where the expression of the *Adi1p* enzyme is unnecessary. In addition, Rnt1p cleavage eliminates the accumulation of 3'-unprocessed species, as shown by the accumulation of 3'-extended and -dicistronic forms of the *ADI1* transcripts observed both in cells lacking Rnt1p or expressing a deletion of the short stem loop structure.

#### DISCUSSION

In this study, we show that the expression of the *ADI1* gene encoding the yeast ARD enzyme is regulated post-transcriptionally by RNase III cleavage and that multiple ribonucleolytic pathways contribute to the control of the steady-state levels of this mRNA. In addition, we show that the *ADI1* mRNA is induced in heat shock conditions. These results provide important advances in our understanding of the regulation of the expression of this class of enzymes. The regulation of the expression of ARD enzymes is an important biomedical problem, as the mammalian ARD gene *ALP1* has been shown to be down-regulated in prostate cancer cells, and its overexpression inhibits prostate cancer cell proliferation (4). In yeast, the *ADI1* mRNA is cleaved by Rnt1p in a bipartite structure found in the open reading frame (Fig. 3). Rnt1p cleavage is normally followed by exonuclease digestion (8, 9, 30). In some cases, Rnt1p cleavage products can be detected when exonuclease mutants are inactivated (8, 9, 30). We did not detect such cleavage products in the case of *ADI1* (Fig. 4). It is possible that the overall low levels of expression of this gene makes the detection of cleavage intermediates difficult.

Our results show that Rnt1p cleavage of the *ADI1* mRNA

serves two purposes. First, cleavage and degradation reduces steady-state levels of the *ADI1* mRNA to avoid expression of the enzyme when unnecessary. Because the *ADI1* mRNA is shown in this study to be highly expressed in heat shock conditions, it is likely that Rnt1p cleavage occurs at normal growth temperatures and that a strong transcriptional induction under heat shock conditions overrides the steady-state levels of cleavage by Rnt1p. In addition, Rnt1p cleavage plays a role in the surveillance of incorrectly processed species. For example, 3'-extended and dicistronic *ADI1-YMR010W* species accumulate in the absence of Rnt1p. These species are also observed, but at lower abundance, in wild-type strains (Fig. 2B), suggesting that the 3'-processing of this gene is intrinsically inefficient. Therefore, cells have adopted ways to eliminate RNA species that contain aberrantly processed species. Rnt1p cleavage contributes to the elimination of these aberrant species, but exoribonucleases are involved as well, because these species are observed both in 5' → 3' and 3' → 5' exonuclease mutants (Fig. 4). Thus, these enzymes act as surveillance enzymes for unprocessed species.

Our study provides a functional framework of the regulation of the *ADI1* mRNA, where expression of the gene is prevented by ribonucleases degradation until a burst of expression occurs under heat shock conditions. This heat shock induction occurs in a mechanism that is independent from Rnt1p cleavage, because an increase of expression is also observed in cells lacking Rnt1p (Fig. 5) in heat shock conditions. Thus, it is likely that this burst of induction occurs by transcriptional induction. Because most of the ribonucleases that are involved in the surveillance of the *ADI1* mRNA are nuclear (Rnt1p, Rat1p, Rrp6p), it is likely that the strong transcriptional induction is followed by a rapid export out of the nucleus, leaving most of the *ADI1* transcripts unaffected by nuclear degradation. Some of these transcripts are however cleaved in heat shock conditions, as the absence of Rnt1p or the deletion of the stem loop structure increases *ADI1* mRNA levels during heat shock (Fig. 5). At this point, we do not know what is the precise status of export of the *ADI1* mRNA and whether its export mechanism is similar to that of heat shock mRNAs.

Finally, it is interesting to consider why more *Adi1p* enzyme may be required in heat shock conditions. The major source of methylthioadenosine is polyamine synthesis, from which it is generated as a side product (Fig. 1); thus, if polyamines are synthesized more rapidly under heat shock conditions, then more methylthioadenosine would be generated that would need to be regenerated by the salvage pathway (Fig. 1). An additional source of methylthioadenosine is the non-enzymatic degradation of *S*-adenosylmethionine (31). Elevated temperatures, such as a switch from 25 to 37 or 42 °C would be expected to increase the non-enzymatic rate of formation of methylthioadenosine from *S*-adenosylmethionine and might also result in the need to up-regulate the salvage pathway. In either case, if the steps catalyzed by the ARD enzymes are rate-limiting in the salvage pathway, increasing the amount of ARD enzyme would respond to the increased demand for this metabolic pathway. Another possibility is that the ARD proteins, which are activated or more active during heat shock conditions, are involved in other metabolic pathway(s). Further studies on the regulation of the methionine salvage pathway and on the metabolic role(s) of ARD enzymes should answer these questions.

*Acknowledgments*—We thank M. Danin-Kreiselman for help in the initial stage of this project, Dr. S. Clarke and members of the Chanfreau Laboratory for helpful discussions, and A. Lee and C. Lee for critical reading of the manuscript.

## REFERENCES

1. Dai, Y., Pochapsky, T. C., and Abeles, R. H. (2001) *Biochemistry* **40**, 6379–6387
2. Wray, J. W., and Abeles, R. H. (1995) *J. Biol. Chem.* **270**, 3147–3153
3. Verma, A., Hirsch, D. J., Glatt, C. E., Ronnett, G. V., and Snyder, S. H. (1993) *Science* **259**, 381–384
4. Oram, S., Jiang, F., Cai, X., Haleem, R., Dincer, Z., and Wang, Z. (2004) *Endocrinology* **145**, 1933–1942
5. Abou Elela, S., Igel, H., and Ares, M., Jr. (1996) *Cell* **85**, 115–124
6. Chanfreau, G., Elela, S. A., Ares, M., Jr., and Guthrie, C. (1997) *Genes Dev.* **11**, 2741–2751
7. Chanfreau, G., Legrain, P., and Jacquier, A. (1998) *J. Mol. Biol.* **284**, 975–988
8. Lee, C. Y., Lee, A., and Chanfreau, G. (2003) *RNA (N. Y.)* **9**, 1362–1370
9. Danin-Kreiselman, M., Lee, C. Y., and Chanfreau, G. (2003) *Mol. Cell* **11**, 1279–1289
10. Ge, D., Lamontagne, B., and Elela, S. A. (2005) *Curr. Biol.* **15**, 140–145
11. Lee, A., Henras, A. K., and Chanfreau, G. (2005) *Mol. Cell.* **19**, 39–51
12. Chanfreau, G., Rotondo, G., Legrain, P., and Jacquier, A. (1998) *EMBO J.* **17**, 3726–3737
13. Petfalski, E., Dandekar, T., Henry, Y., and Tollervey, D. (1998) *Mol. Cell. Biol.* **18**, 1181–1189
14. van Hoof, A., Lennertz, P., and Parker, R. (2000) *EMBO J.* **19**, 1357–1365
15. Storici, F., Lewis, L. K., and Resnick, M. A. (2001) *Nat. Biotechnol.* **19**, 773–776
16. Pochapsky, T. C., Pochapsky, S. S., Ju, T., Mo, H., Al-Mjeni, F., and Maroney, M. J. (2002) *Nat. Struct. Biol.* **9**, 966–972
17. Subhi, A. L., Diegelman, P., Porter, C. W., Tang, B., Lu, Z. J., Markham, G. D., and Kruger, W. D. (2003) *J. Biol. Chem.* **278**, 49868–49873
18. Chanfreau, G., Buckle, M., and Jacquier, A. (2000) *Proc. Natl. Acad. Sci. U. S. A.* **97**, 3142–3147
19. Chanfreau, G. (2003) *Eukaryotic Cell* **2**, 901–909
20. Zuker, M. (2003) *Nucleic Acids Res.* **31**, 3406–3415
21. Mathews, D. H., Sabina, J., Zuker, M., and Turner, D. H. (1999) *J. Mol. Biol.* **288**, 911–940
22. Nagel, R., and Ares, M., Jr. (2000) *RNA (N. Y.)* **6**, 1142–1156
23. Wu, H., Henras, A., Chanfreau, G., and Feigon, J. (2004) *Proc. Natl. Acad. Sci. U. S. A.* **101**, 8307–8312
24. Franch, T., Thisted, T., and Gerdes, K. (1999) *J. Biol. Chem.* **274**, 26572–26578
25. Wu, H., Yang, P. K., Butcher, S. E., Kang, S., Chanfreau, G., and Feigon, J. (2001) *EMBO J.* **20**, 7240–7249
26. Johnson, A. W. (1997) *Mol. Cell. Biol.* **17**, 6122–6130
27. Allmang, C., Kufel, J., Chanfreau, G., Mitchell, P., Petfalski, E., and Tollervey, D. (1999) *EMBO J.* **18**, 5399–5410
28. van Hoof, A., Lennertz, P., and Parker, R. (2000) *Mol. Cell. Biol.* **20**, 441–452
29. Gasch, A. P., Spellman, P. T., Kao, C. M., Carmel-Harel, O., Eisen, M. B., Storz, G., Botstein, D., and Brown, P. O. (2000) *Mol. Biol. Cell* **11**, 4241–4257
30. Qu, L. H., Henras, A., Lu, Y. J., Zhou, H., Zhou, W. X., Zhu, Y. Q., Zhao, J., Henry, Y., Caizergues-Ferrer, M., and Bachelier, J. P. (1999) *Mol. Cell. Biol.* **19**, 1144–1158
31. Hoffman, J. L. (1986) *Biochemistry* **25**, 4444–4449